

Supporting Information for

**SAM: Self-adapting Mixture Prior to Dynamically Borrow  
Information from Historical Data in Clinical Trials**

by

Peng Yang, Yuansong Zhao, Lei Nie, Jonathon Vallejo, Ying Yuan

## Web Appendix A

### A.1. Proof of theorem 1

When  $n_h \rightarrow \infty$ ,  $\hat{\theta}_h \rightarrow \theta$ . Since the likelihood ratio test is consistent, when  $D_h$  and  $D$  are congruent (i.e.,  $\theta = \theta_h$ ),  $\frac{p(D|\theta=\hat{\theta}_h)}{p(D|\theta=\hat{\theta}_h+\delta)} \rightarrow \infty$  and  $\frac{p(D|\theta=\hat{\theta}_h)}{p(D|\theta=\hat{\theta}_h-\delta)} \rightarrow \infty$ , so  $R \rightarrow \infty$  and  $w = \frac{R}{1+R} \rightarrow 1$ . As a result,  $\pi_{sam}(\theta) \rightarrow \pi_1(\theta)$ .

When  $D_h$  and  $D$  are incongruent (i.e.,  $\theta = \theta_h + \delta$  or  $\theta = \theta_h - \delta$ ),  $\frac{p(D|\theta=\hat{\theta}_h)}{\max\{p(D|\theta=\hat{\theta}_h+\delta), p(D|\theta=\hat{\theta}_h-\delta)\}} \rightarrow 0$ , so  $R \rightarrow 0$  and  $w = \frac{R}{1+R} \rightarrow 0$ . As a result,  $\pi_{sam}(\theta) \rightarrow \pi_0(\theta)$ .

## Web Appendix B

### Results for sensitivity analysis

#### B.1. Operating characteristics when the clinically significant difference $\delta = 0.15$

We studied the operating characteristics of self-adapting mixture (SAM) priors, in comparison to the fixed-weight mixture prior with  $\tilde{w} = 0.5$  (Mix50), power prior (PP), and commensurate prior (CP), when the clinically significant difference (CSD)  $\delta = 0.15$ . The endpoint is binary. We generated historical data  $D_h$  from *Bernoulli* ( $\theta_h$ ) with  $\theta_h = 0.4, 0.3, 0.2$ , and sample size  $n_h = 150$  for all three cases. When  $\theta_h = 0.4, 0.3$ , and  $0.2$ , the sample sizes for the control arm and treatment arm were set as  $n = 75, 75, 60$ , and  $n_t = 150, 150, 120$ , respectively. The sample sizes were chosen such that the power of the methods under comparison was mostly in the range of 70% to 90%. Figure S1 shows the relative bias and relative mean square error (RMSE), and Table S1 shows the type I error rate and power based on 2000 simulations.

**FIGURE S1.** (A) Relative bias and (B) relative mean square error (RMSE) for the posterior mean estimate of  $\theta$  for the SAM prior, mixture prior with  $\tilde{w} = 0.5$  (Mix50), a power prior (PP), and a commensurate prior (CP) for a binary endpoint, with a non-informative prior (NP) as reference. The vertical dotted line indicates  $\theta = \theta_h$ .

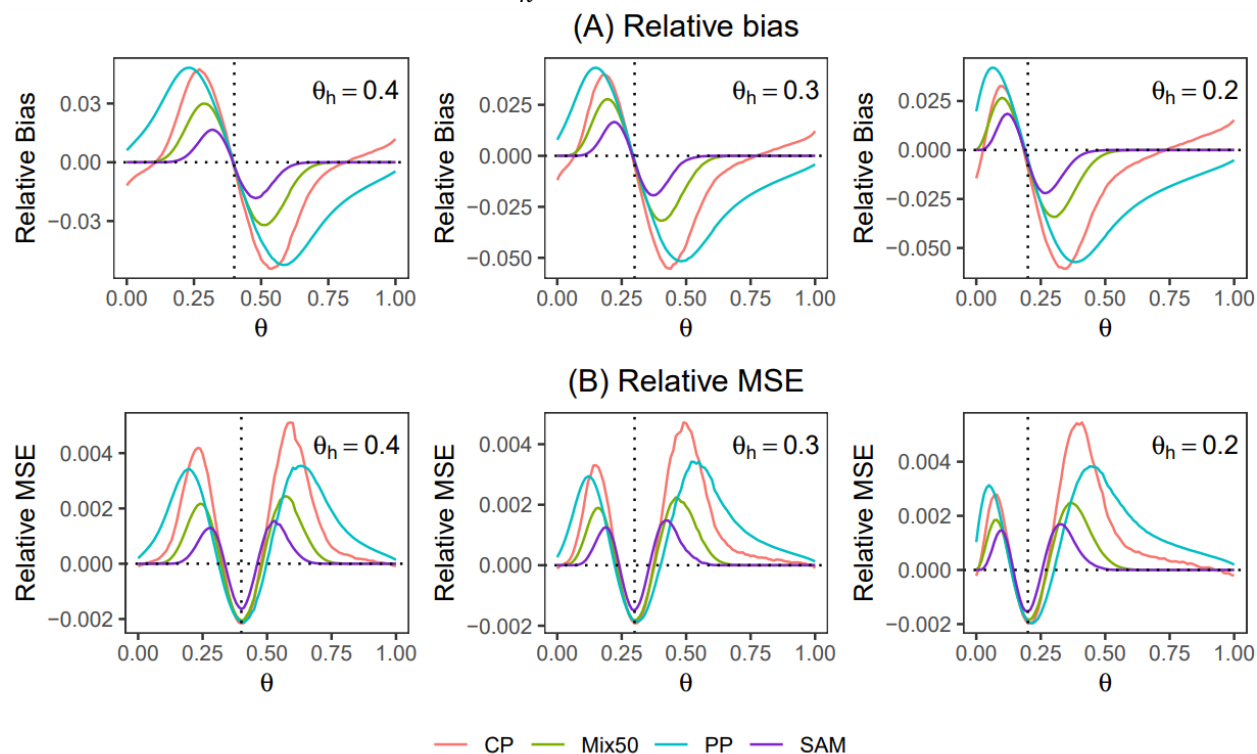


**TABLE S1.** Type I error and power when using a noninformative prior (NP), a SAM prior with  $\delta = 0.15$ , a mixture prior with  $\tilde{w} = 0.5$  (Mix50), a power prior (PP), and a commensurate prior (CP) with a binary endpoint.

Scenario	$\theta_c$	$\theta_t$	NP	SAM	Mix50	PP	CP
<b>Case 1: <math>\theta_h = 0.4</math></b>							
<b>Congruent</b>							
1.1*	0.4	0.4	0.050	0.050	0.050	0.051	0.050
1.2	0.4	0.55	0.683	0.876	0.904	0.905	0.904
1.3	0.41	0.56	0.678	0.874	0.911	0.912	0.906
1.4	0.38	0.53	0.698	0.875	0.883	0.877	0.856
<b>Incongruent</b>							
1.5*	0.55	0.55	0.05	0.132	0.208	0.272	0.296
1.6*	0.6	0.6	0.052	0.076	0.138	0.267	0.219
1.7	0.25	0.4	0.735	0.712	0.588	0.54	0.452
1.8	0.2	0.35	0.768	0.788	0.682	0.529	0.478
<b>Case 2: <math>\theta_h = 0.3</math></b>							
<b>Congruent</b>							
2.1*	0.3	0.3	0.050	0.051	0.051	0.051	0.051
2.2	0.3	0.45	0.722	0.897	0.921	0.91	0.934
2.3	0.31	0.46	0.716	0.889	0.921	0.916	0.941
2.4	0.28	0.43	0.733	0.902	0.906	0.886	0.897
<b>Incongruent</b>							
2.5*	0.45	0.45	0.05	0.12	0.173	0.27	0.288
2.6*	0.5	0.5	0.055	0.078	0.128	0.27	0.214
2.7	0.15	0.3	0.823	0.786	0.688	0.636	0.538
2.8	0.1	0.25	0.897	0.894	0.823	0.666	0.7
<b>Case 3: <math>\theta_h = 0.2</math></b>							
<b>Congruent</b>							
3.1*	0.2	0.2	0.051	0.050	0.051	0.051	0.051
3.2	0.2	0.35	0.693	0.882	0.906	0.927	0.916
3.3	0.21	0.36	0.691	0.886	0.906	0.93	0.926
3.4	0.18	0.33	0.706	0.904	0.902	0.904	0.88
<b>Incongruent</b>							
3.5*	0.35	0.35	0.052	0.128	0.183	0.303	0.313
3.6*	0.4	0.4	0.053	0.082	0.122	0.298	0.22
3.7	0.05	0.2	0.892	0.888	0.765	0.702	0.662
3.8	0.03	0.18	0.952	0.945	0.936	0.737	0.806

\*Type I error.

## B.2. Operating characteristics when an informative prior for the probability of prior-data conflict is used

We considered the case that investigators believe a priori that there is a 70% or 90% chance that  $D_h$  is congruent to  $D$ . Accordingly, we set  $\tilde{w} = 0.7$  or  $0.9$  in the fixed-weight mixture prior and set prior odds = 7/3 or 9/1 in the SAM prior. We considered both binary endpoint and normal endpoints. The simulation setup is the same as the main simulation (Section 3.1) described in the paper. Figure S2 shows the relative bias and RMSE, and Table S2 shows the type I error rate and power for a binary endpoint. Figure S3 and Table S3 show the results for a normal endpoint.

**FIGURE S2.** (A) Relative bias and (B) relative mean square error (RMSE) for the posterior mean estimate of  $\theta$  for a SAM prior with prior odds = 7/3 (SAM 7:3), A SAM prior with prior odds = 9/1 (SAM 9:1), a mixture prior with  $\tilde{w} = 0.7$  (Mix70), and a mixture prior with  $\tilde{w} = 0.9$  (Mix90) for a binary endpoint, with a non-informative prior (NP) as reference. The vertical dotted line indicates  $\theta = \theta_h$ .

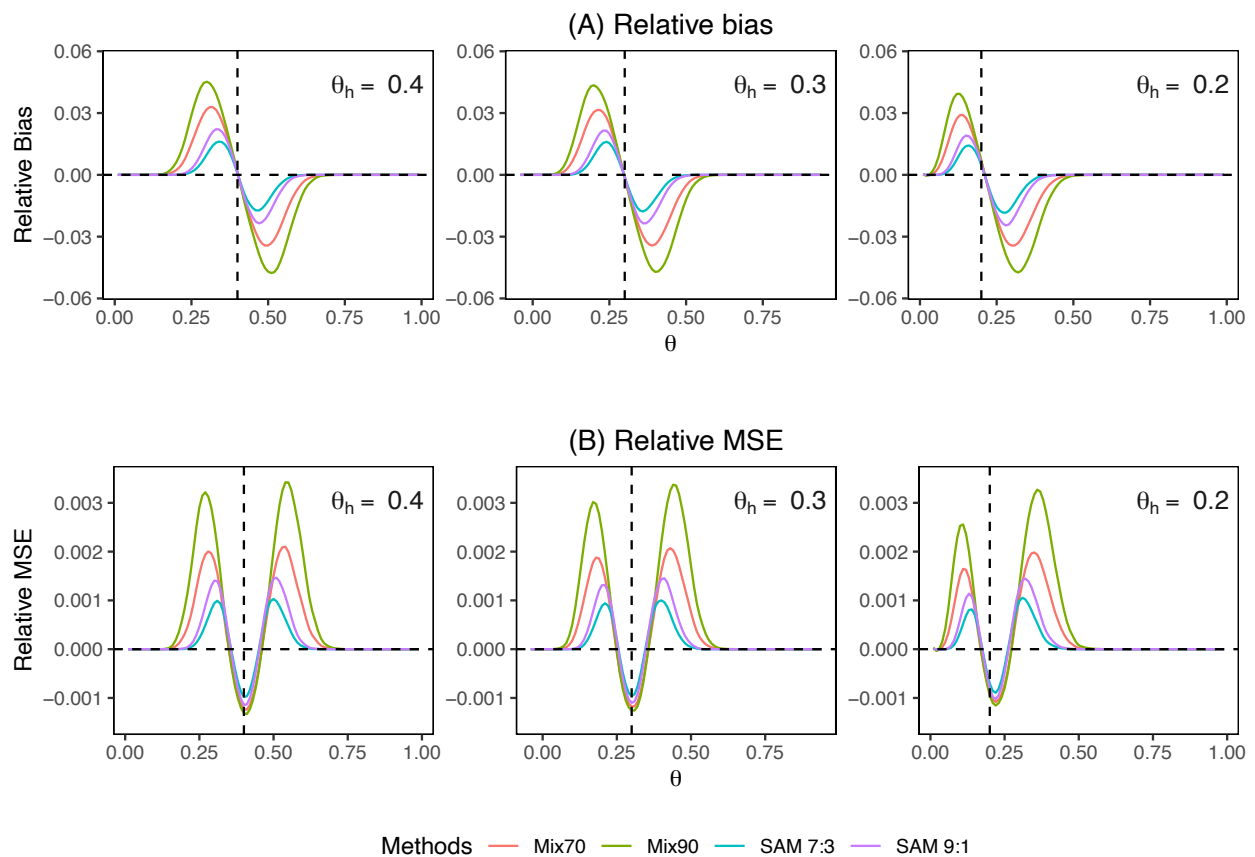


**TABLE S2.** Type I error and power when using a noninformative prior (NP), a SAM prior with prior odds = 7:3 (SAM 7:3), a SAM prior with prior odds = 9:1 (SAM 9:1), a mixture prior with  $\tilde{w} = 0.7$  (Mix70), and a mixture prior with  $\tilde{w} = 0.9$  (Mix90) for a binary endpoint.

Scenario	$\theta_c$	$\theta_t$	NP	SAM 7:3	Mix70	SAM 9:1	Mix90
<b>Case 1: <math>\theta_h = 0.4</math></b>							
<b>Congruent</b>							
1.1*	0.4	0.4	0.051	0.050	0.050	0.051	0.050
1.2	0.4	0.5	0.636	0.885	0.914	0.912	0.933
1.3	0.41	0.51	0.655	0.885	0.922	0.918	0.940
1.4	0.38	0.48	0.636	0.836	0.850	0.847	0.861
<b>Incongruent</b>							
1.5*	0.5	0.5	0.056	0.171	0.290	0.247	0.437
1.6*	0.55	0.55	0.056	0.099	0.198	0.122	0.307
1.7	0.3	0.4	0.657	0.609	0.431	0.574	0.356
1.8	0.25	0.35	0.69	0.748	0.542	0.746	0.397
<b>Case 2: <math>\theta_h = 0.3</math></b>							
<b>Congruent</b>							
2.1*	0.3	0.3	0.050	0.050	0.050	0.050	0.050
2.2	0.3	0.4	0.657	0.899	0.924	0.925	0.947
2.3	0.31	0.41	0.649	0.906	0.943	0.936	0.965
2.4	0.28	0.38	0.667	0.855	0.876	0.876	0.897
<b>Incongruent</b>							
2.5*	0.4	0.4	0.048	0.188	0.298	0.234	0.439
2.6*	0.45	0.45	0.049	0.083	0.164	0.104	0.252
2.7	0.2	0.3	0.720	0.679	0.486	0.643	0.402
2.8	0.17	0.27	0.773	0.786	0.553	0.772	0.405
<b>Case 3: <math>\theta_h = 0.2</math></b>							
<b>Congruent</b>							
3.1*	0.2	0.2	0.051	0.050	0.051	0.051	0.051
3.2	0.2	0.3	0.698	0.921	0.938	0.921	0.952
3.3	0.21	0.31	0.696	0.915	0.939	0.915	0.960
3.4	0.18	0.28	0.707	0.890	0.899	0.890	0.913
<b>Incongruent</b>							
3.5*	0.3	0.3	0.058	0.192	0.308	0.256	0.440
3.6*	0.35	0.35	0.054	0.102	0.193	0.126	0.293
3.7	0.1	0.2	0.832	0.787	0.585	0.747	0.496
3.8	0.07	0.17	0.898	0.922	0.736	0.914	0.598

\*Type I error.

**FIGURE S3.** (A) Relative bias and (B) relative mean square error (RMSE) for the posterior mean estimate of  $\theta$  for a SAM prior with prior odds = 7/3 (SAM 7:3), A SAM prior with prior odds = 9/1 (SAM 9:1), a mixture prior with  $\tilde{w} = 0.7$  (Mix70), and a mixture prior with  $\tilde{w} = 0.9$  (Mix90) for a continuous endpoint, with a non-informative prior (NP) as reference. The vertical dotted line indicates  $\theta = \theta_h$ .

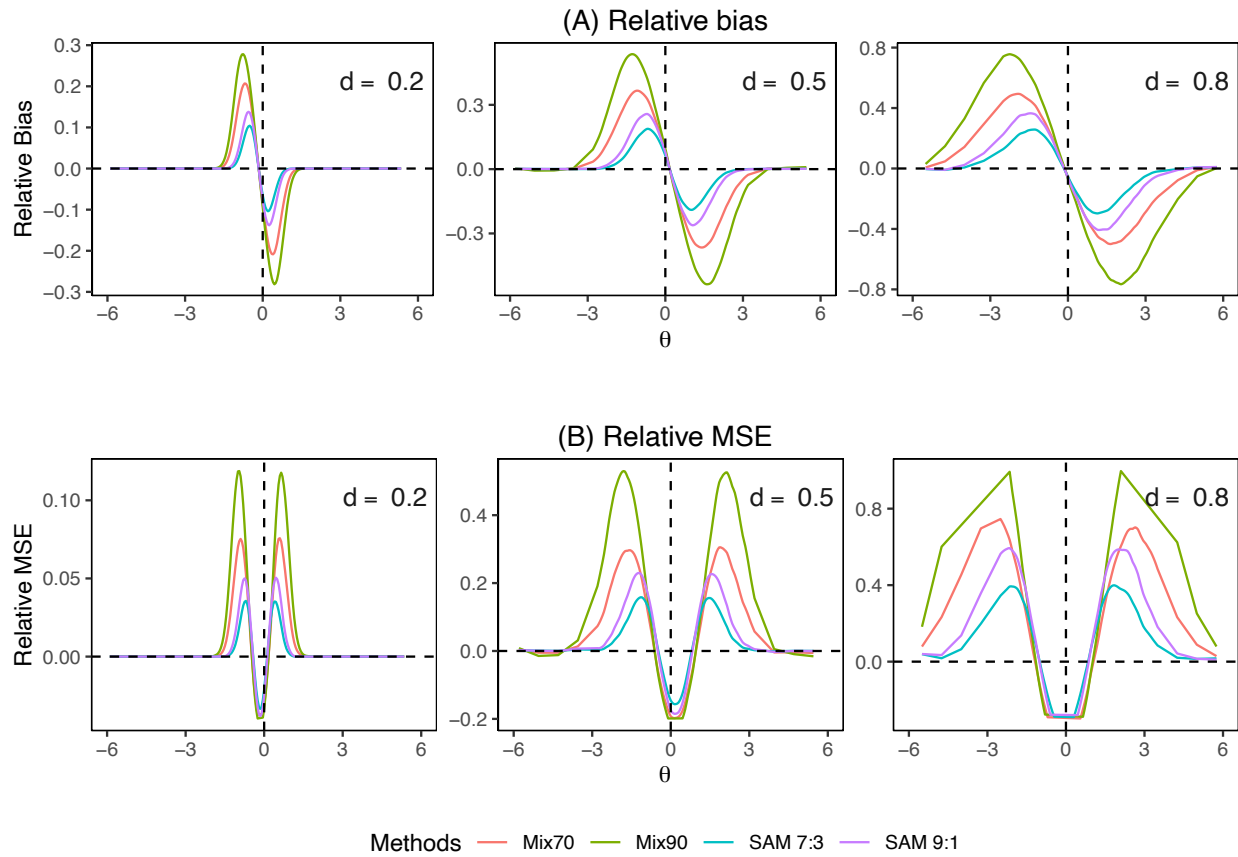


**TABLE S3.** Type I error and power when using a noninformative prior (NP), a SAM prior with prior odds = 7:3 (SAM 7:3), a SAM prior with prior odds = 9:1 (SAM 9:1), a mixture prior with  $\tilde{w} = 0.7$  (Mix70), and a mixture prior with  $\tilde{w} = 0.9$  (Mix90) for a continuous endpoint.

Scenario	$\theta_c$	$\theta_t$	NP	SAM 7:3	Mix70	SAM 9:1	Mix90
<b>Case 1: small effect size <math>d = 0.2</math></b>							
<b>Congruent</b>							
1.1*	0	0	0.051	0.051	0.050	0.051	0.051
1.2	0	0.6	0.712	0.894	0.933	0.922	0.952
1.3	-0.1	0.5	0.712	0.890	0.906	0.906	0.915
1.4	0.1	0.7	0.712	0.868	0.931	0.907	0.963
<b>Incongruent</b>							
1.5*	0.6	0.6	0.046	0.131	0.229	0.175	0.363
1.6*	0.9	0.9	0.046	0.057	0.106	0.067	0.172
1.7	-0.6	0	0.709	0.569	0.402	0.514	0.351
1.8	-0.9	-0.3	0.708	0.681	0.406	0.655	0.289
<b>Case 2: medium effect size <math>d = 0.5</math></b>							
<b>Congruent</b>							
2.1*	0	0	0.051	0.051	0.050	0.051	0.051
2.2	0	1.5	0.736	0.915	0.939	0.934	0.956
2.3	-0.2	1.3	0.734	0.887	0.912	0.897	0.928
2.4	0.1	1.6	0.737	0.940	0.956	0.953	0.971
<b>Incongruent</b>							
2.5*	1.5	1.5	0.052	0.213	0.325	0.279	0.474
2.6*	1.8	1.8	0.052	0.143	0.271	0.196	0.410
2.7	-1.5	0	0.724	0.715	0.565	0.678	0.463
2.8	-1.8	-0.3	0.722	0.744	0.583	0.723	0.470
<b>Case 3: large effect size <math>d = 0.8</math></b>							
<b>Congruent</b>							
3.1*	0	0	0.051	0.051	0.051	0.052	0.051
3.2	0	2.4	0.708	0.880	0.893	0.903	0.933
3.3	-0.3	2.1	0.704	0.879	0.884	0.899	0.908
3.4	0.1	2.5	0.708	0.880	0.900	0.911	0.937
<b>Incongruent</b>							
3.5*	2.4	2.4	0.064	0.094	0.138	0.128	0.227
3.6*	2.7	2.7	0.066	0.071	0.120	0.098	0.203
3.7	-2.4	0	0.678	0.627	0.492	0.579	0.415
3.8	-2.7	-0.3	0.672	0.636	0.482	0.597	0.380

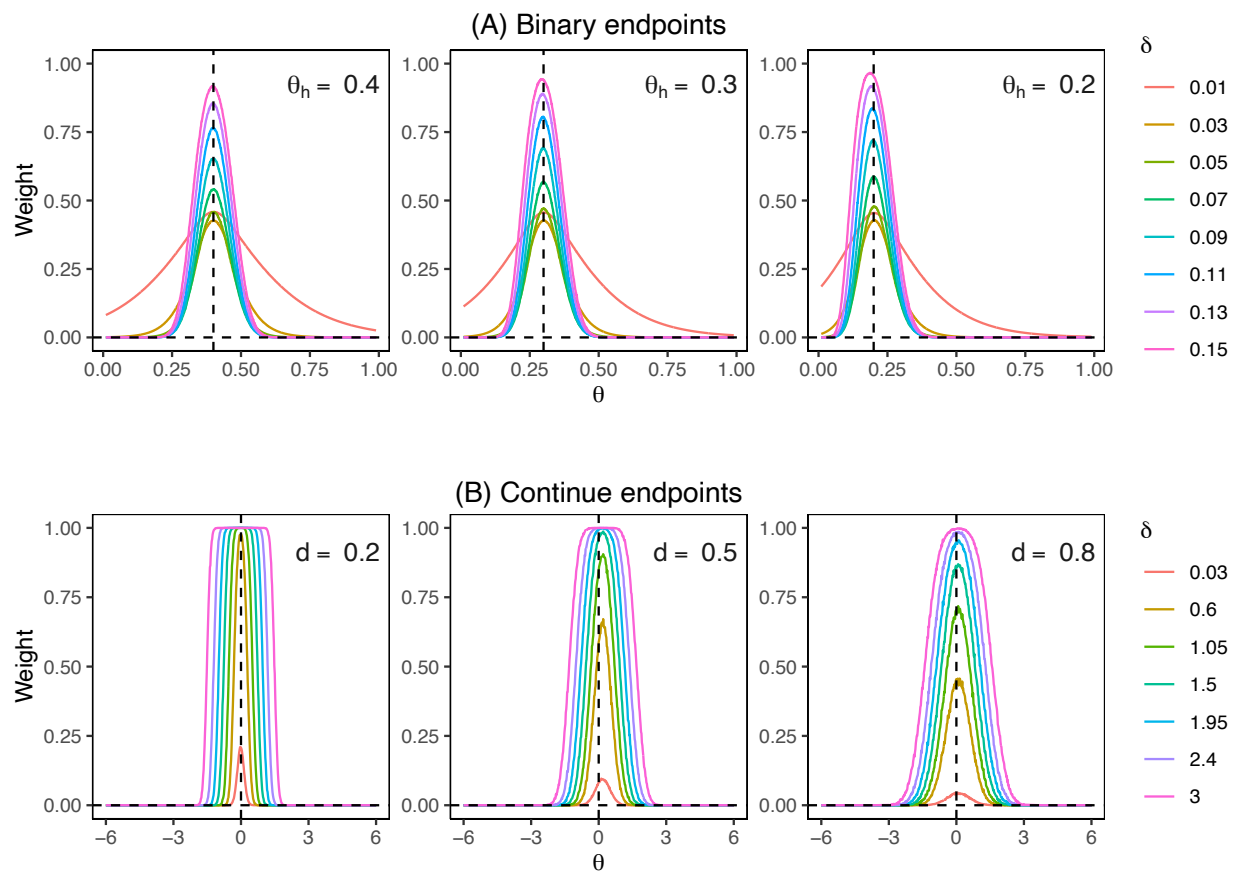
\*Type I Error; Effective size  $d = (\theta_t - \theta)/\sigma$ .



### B.3. The mixture weight in the SAM prior in relation to clinically significant difference $\delta$

In order to evaluate the sensitivity of the SAM prior, we investigated the change of the mixture weight  $w$  in relation to the CSD, for both binary and continuous endpoints. Our simulation setup closely mirrors the one described in the main simulation (Section 3.1) of the paper. For the binary case, we utilized a grid of  $\delta$  values ranging from 0.01 to 0.15, with a step size of 0.02. Meanwhile, the continuous case used a grid of  $\delta$  values  $\{0.01, 0.2, 0.35, 0.5, 0.65, 0.8, 1\}\sigma$ , where  $\sigma = 3$ , consistent with the main text simulation setting. Figure S4 illustrates the changes in mixture weights associated with varying degrees of prior-data conflicts. Our findings suggest that the mixture weights are concentrated within the CSD and decrease significantly as the level of prior-data conflicts increases.

**FIGURE S4.** Mixture weight of the SAM prior under different degrees of prior-data conflict (i.e.,  $\theta - \theta_h$ ) and CSD (i.e.,  $\delta$ ) for binary and continuous endpoints. The vertical dotted line indicates  $\theta = \theta_h$ .



## Web Appendix C

### Operating characteristics of the fully Bayesian mixture prior and fixed-weight mixture priors using bimodal prior

The SAM prior is an empirical Bayes method as  $w$  depends on the trial  $D$ . Additionally, we investigated the operating characteristics of three alternative approaches: (a) a fully Bayesian approach by assigning  $w$  a uniform prior, and two modifications of the fixed-weight mixture prior by assigning  $\pi_0(\theta)$  a bimodal prior including (b) the inverse moment (iMOM) prior (Johnson and Rossell, 2010) and (c) a mixture of two beta/normal priors with modes centered at  $\theta_h - \delta$  and  $\theta_h + \delta$  (Figure S5).

Methods (b) and (c) are designed to account for  $H_1$  and CSD in the fixed-weight mixture prior. Specifically, we investigated the bimodal beta/normal prior with  $\tilde{w} = 0.5$  (bMix50) for binary and continuous endpoints, respectively, and the non-local inverse moment (iMOM) prior with  $\tilde{w} = 0.5$  (iMix50) as  $\pi_0(\theta)$ . The non-local iMOM balances the convergence rates of evidence gain with null and alternative hypotheses as the sample size increases. The iMOM prior is defined as follows:

$$\pi_I(\theta; \theta_0, k, v, \tau) = \frac{k\tau^v}{\Gamma(v/2k)} [(\theta - \theta_0)^2]^{-\frac{v+1}{2}} \exp\left\{-\left[\left(\frac{\theta - \theta_0}{\tau}\right)^2\right]^{-k}\right\}.$$

This density function has two modes at

$$\hat{\theta} = \theta_0 \pm \tau \left[\frac{2k}{v+1}\right]^{1/2k}.$$

We used  $k = 1$  and  $v = 2$  to back-solve for the corresponding  $\tau$  values, ensuring that the modes of the bimodal priors are centered at  $\theta_h - \delta$  and  $\theta_h + \delta$  for a given  $\delta$ . We then evaluated the performance of the two bimodal prior approaches and compared them to SAM priors. The simulation setup was the same as the main simulation described in Section 3.1 of the main text, and we obtained the posterior mean estimates of  $\theta$  using importance sampling.

Simulation results show that none of the three methods perform as well as the SAM prior. The fully Bayesian approach assigning  $w$  a uniform prior has substantial and persistent bias even when prior-data conflict is large. In addition, it has the largest MSE when there is no or large prior-data conflict. Compared to the SAM prior, the two modifications of the fixed-weight mixture prior have substantially larger relative bias and mean squared errors (MSEs) as prior-data conflict increases (see Figures S6-7). The poor performance of bimodal priors can be attributed to the fact that the probability mass outside the two modes,  $\theta_h - \delta$  and  $\theta_h + \delta$ , is low. This resulted in the likelihood of historical data dominating the posterior inference outside this range, leading to substantial bias in the estimates.

**FIGURE S5.** An example of a bimodal beta distribution (orange line) and an iMOM distribution (pink line). The vertical dotted line indicates  $\theta = \theta_h \pm \delta$  with  $\delta = 0.1$ .

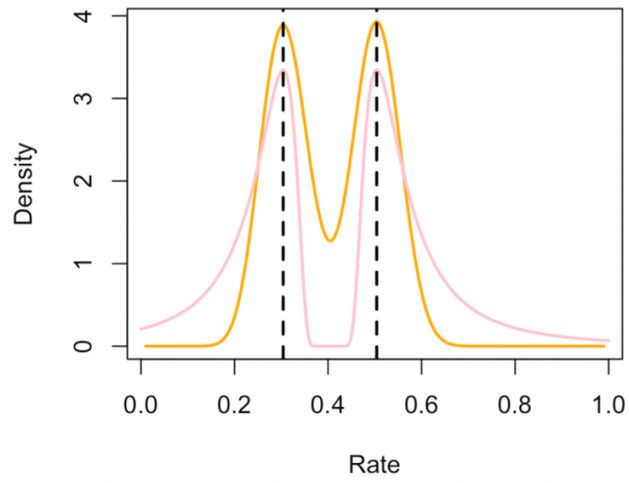


**FIGURE S6.** (A) Relative bias and (B) relative mean square error (RMSE) of the posterior mean estimate of  $\theta$ , with a non-informative prior (NP) as the reference, for a SAM prior, the fully Bayesian mixture prior with a uniform prior on  $w$  (uMix), the fixed-weight mixture prior assigning  $\pi_0(\theta)$  a bimodal beta prior with  $\tilde{w} = 0.5$  (bMix50), and the fixed-weight mixture prior assigning  $\pi_0(\theta)$  an iMOM prior with  $\tilde{w} = 0.5$  (iMix50), for a binary endpoint. The vertical dotted line indicates  $\theta = \theta_h$ .

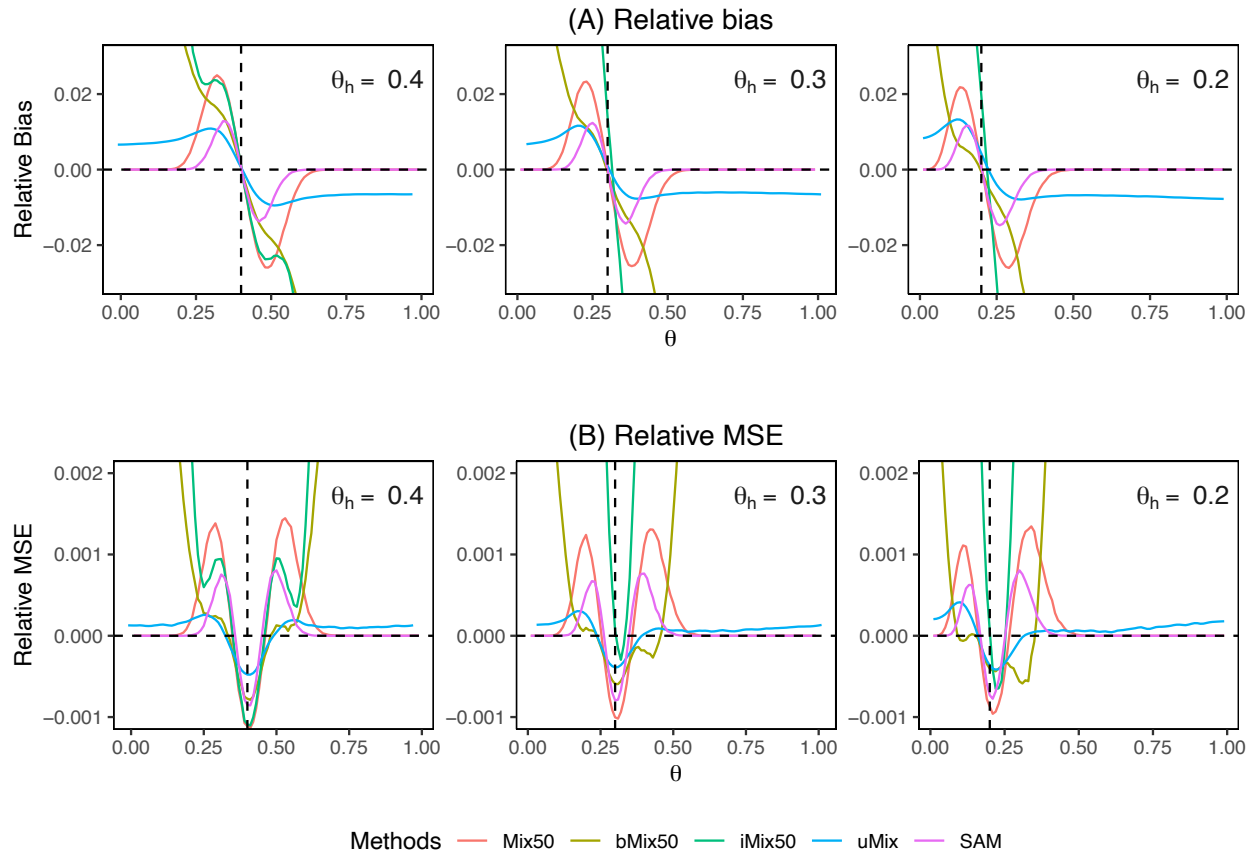
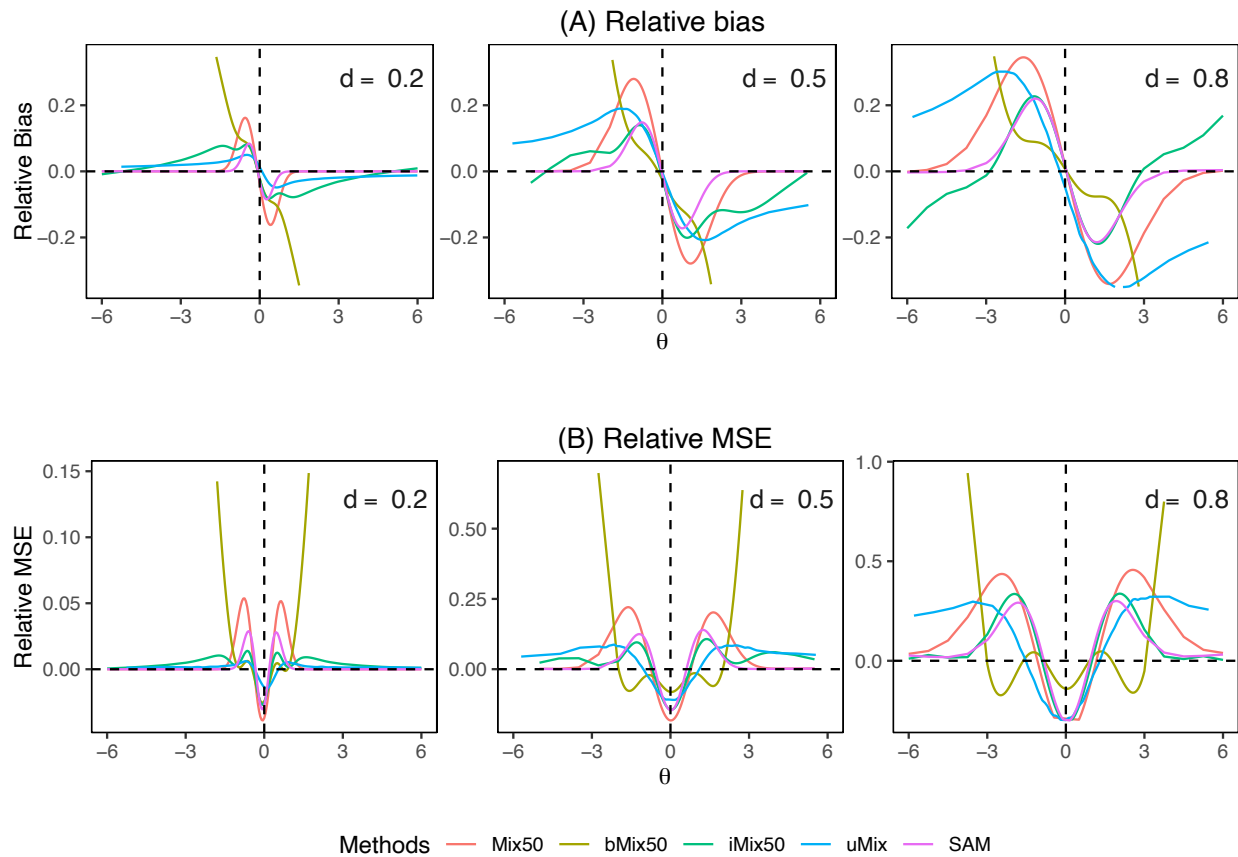


**FIGURE S7.** (A) Relative bias and (B) relative mean square error (RMSE) of the posterior mean estimate of  $\theta$ , with a non-informative prior (NP) as the reference, for a SAM prior, the fully Bayesian mixture prior with a uniform prior on  $w$  (uMix), the fixed-weight mixture prior assigning  $\pi_0(\theta)$  a bimodal beta prior with  $\tilde{w} = 0.5$  (bMix50), and the fixed-weight mixture prior assigning  $\pi_0(\theta)$  an iMOM prior with  $\tilde{w} = 0.5$  (iMix50), for a continuous endpoint. The vertical dotted line indicates  $\theta = \theta_h$ .



## Web Appendix D

### SAM priors for survival endpoints

In this section, we introduce how to apply SAM prior to survival endpoints. Assume historical data  $D_h$  consisting of  $T_{h1}, T_{h2}, \dots, T_{hn_h} \sim \exp(\lambda_h)$ , subject to non-informative right censoring  $C_{h1}, C_{h2}, \dots, C_{hn_h}$ . Let  $U_{hi} = \min(C_{hi}, t_{hi})$  denote the observed time, and  $\delta_{hi} = I(T_{hi} < C_{hi})$  denote the censoring indicator. Let  $\lambda$  denote the hazard of the current trial control. Given a non-informative gamma prior,  $\lambda \sim \text{Gamma}(\alpha, \beta)$ , e.g.,  $\alpha = \beta = 0.1$ , the informative prior that incorporates historical information is given by:

$$\pi_1(\lambda) = \text{Gamma}(\alpha + r_h, \beta + Q_h),$$

where  $r_h = \sum_{i=1}^{n_h} \delta_{hi}$  and  $Q_h = \sum_{i=1}^{n_h} u_{hi}$  represent the number of events and the total observed time, respectively. The SAM prior arises as

$$\pi_{sam}(\lambda) = w \text{Gamma}(\alpha + r_h, \beta + Q_h) + (1 - w) \text{Gamma}(\alpha, \beta),$$

where  $w = \frac{R}{1+R}$  with

$$R = \frac{\hat{\lambda}_h^r \exp\{-\hat{\lambda}_h Q\}}{\max\{(\hat{\lambda}_h - \delta)^r \exp\{-(\hat{\lambda}_h - \delta)Q\}, (\hat{\lambda}_h + \delta)^r \exp\{-(\hat{\lambda}_h + \delta)Q\}\}},$$

where  $\hat{\lambda}_h = (\alpha + r_h)/(\beta + Q_h)$ . Owing to its conjugacy, given  $\pi_{sam}(\lambda)$  and trial data  $D$ , the posterior of  $\lambda$  is given by

$$p(\lambda|D, D_h) = w^* \text{Gamma}(\alpha + r_h + r, \beta + Q_h + Q) + (1 - w^*) \text{Gamma}(\alpha + r, \beta + Q),$$

where  $w^*$  is the re-weighted  $w$  by the posterior normalizing constant associated with each mixture component, given by

$$w^* = \frac{wz_1}{wz_1 + wz_0}, z_0 = \frac{\beta^\alpha \Gamma(\alpha + r)}{\Gamma(\alpha)(\beta + Q)^{\alpha+r}}, z_1 = \frac{(\beta + Q_h)^\alpha \Gamma(\alpha + r + r_h)}{\Gamma(\alpha + r_h)(\beta + Q + Q_h)^{\alpha+r+r_h}}.$$

A similar approach can be applied to a more flexible piecewise exponential model.

We conducted a simulation study to evaluate the operating characteristics of the SAM prior for survival endpoints. We considered three hazards for  $D_h$ , i.e.,  $\lambda_h = 0.5, 1, \text{ and } 2$ , with the sample size  $n_h = 100, 60, \text{ and } 30$ , respectively, and simulated control arm data  $D$  with the sample size  $n = 50, 30, \text{ and } 12$ , respectively. The sample sizes were chosen such that the power of the methods under comparison is mostly in the range of 70% to 90%. For each of the three values of  $\lambda_h$ , we varied the hazard of the current control (i.e.,  $\lambda$ ) to generate different degrees of prior-data conflict, and set  $\delta = 0.1, 0.2, \text{ and } 0.4$  for the three cases. We conducted 2000 simulations for each configuration. We compared the SAM prior with Mix50.

We found that the SAM prior has uniformly smaller relative biases and relative mean squared errors (RMSEs) than Mix50 (Figure S8). Furthermore, Table S4 displays the type I error and power when  $\lambda_h = 1$ ,  $n = n_h = 50$ , and  $n_t = 100$ , which demonstrates that the SAM prior provides more power gain than Mix50 while maintaining reasonable type I error rates.

**FIGURE S8.** (A) Relative bias and (B) relative mean square error (RMSE) of the posterior mean estimate of  $\lambda$  for a SAM prior, a mixture prior with  $\tilde{w} = 0.5$  (Mix50) for a survival endpoint, with a non-informative prior (NP) as reference. The vertical dotted line indicates  $\lambda = \lambda_h$ .

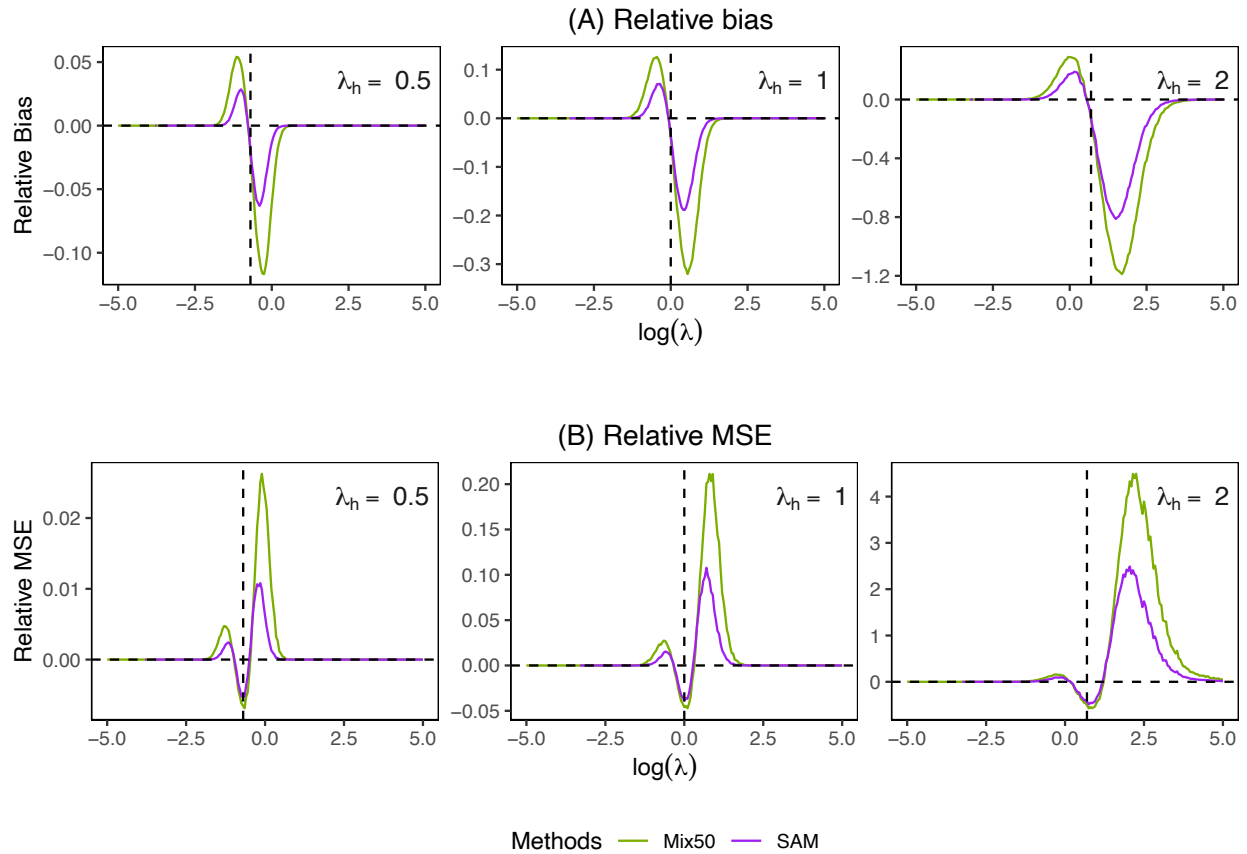


**TABLE S4.** Simulation results for survival endpoints using a noninformative prior (NP), a SAM prior with  $\delta = 0.4$ , a mixture prior with  $\tilde{w} = 0.5$  (Mix50).

Scenario	$\lambda_c$	$\lambda_t$	NP	SAM	Mix50
<b>Congruent</b>					
1*	1.00	1.00	0.052	0.051	0.052
2	1.00	1.60	0.808	0.974	0.720
3	0.90	1.40	0.782	0.876	0.596
4	0.95	1.45	0.739	0.875	0.508
<b>Incongruent</b>					
5*	0.70	0.70	0.053	0.067	0.002
6*	1.30	1.30	0.052	0.154	0.172
7	0.50	1.00	0.967	0.984	0.867
8	0.70	1.20	0.887	0.886	0.434

\*Type I error.



## Web Appendix E

### Ankylosing spondylitis trial data and sensitivity analysis.

Table S5 displays historical data on the placebo from 9 studies. Notably, the study by Baeten (2013) has a small sample size ( $n = 6$ ), which raises concerns about its inclusion in the analysis. As a sensitivity analysis, we redid the analysis by excluding the dataset from Baeten (2013). The resulting MAP prior from the remaining datasets is  $\pi_1(\theta) = 0.64\text{Beta}(39.9,71.6) + 0.35\text{Beta}(7.2,12.4)$ , which is very similar to that obtained when Baeten (2013) was included, i.e.,  $\pi_1(\theta) = 0.63\text{Beta}(42.5,77.2) + 0.37\text{Beta}(7.2,12.4)$ . The mean of the resulting MAP prior is  $\hat{\theta}_h = 0.362$ . Table S6 displays the type I error and power, in comparison with the robust MAP prior with  $\tilde{w} = 0.5$  (Mix50) and 0.9 (Mix90), after excluding Baeten (2013). Additionally, Figure S9 shows the relative bias and RMSE of SAM, Mix50, and Mix90 after excluding Baeten (2013). The findings are comparable to those obtained using all datasets, as shown in Figure 4 and Table 3 in the main text.

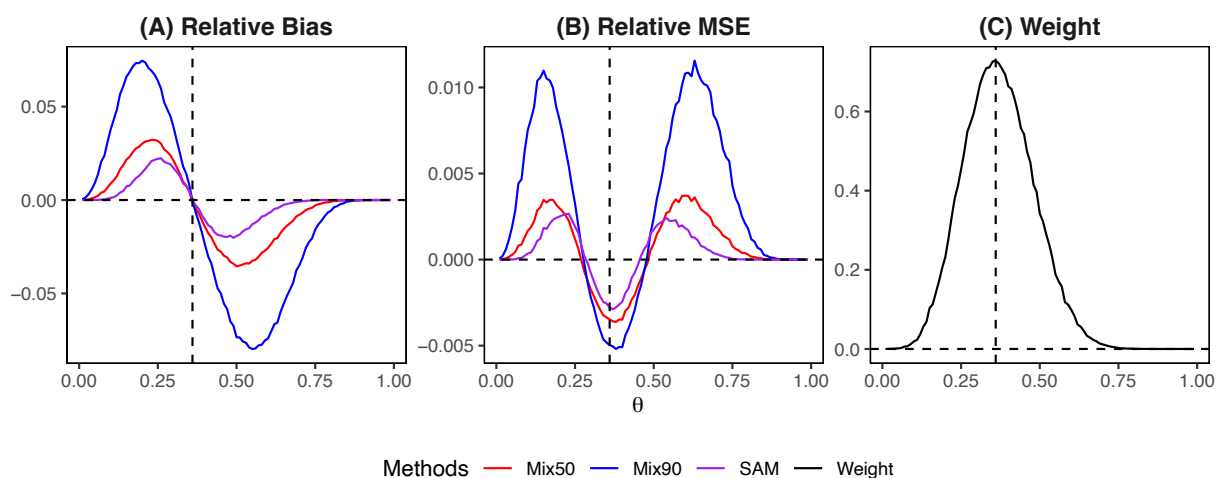
**TABLE S5.** Historical data of placebo arms from nine clinical trials with ASAS20 response as the primary endpoint.

Author/Year	Events	Total
Baeten (2013)	1	6
Deodhar (2016)	35	122
Deodhar (2019)	31	104
Erdes (2019)	10	23
Huang (2019)	56	153
Kivitz (2018)	55	117
Pavelka (2017)	28	76
Sieper (2017)	21	74
van der Heijde (2018)	35	87

**TABLE S6.** Type I error and power of the SAM prior, in comparison with the robust MAP prior with  $\tilde{w} = 0.5$  (Mix50) and 0.9 (Mix90), for ankylosing spondylitis trial with the dataset from Baeten (2013) excluded.

Scenario	$\theta_c$	$\theta_t$	NP	SAM	Mix50	Mix90
<b>Congruent</b>						
1*	0.36	0.36	0.050	0.052	0.051	0.052
2	0.36	0.56	0.620	0.819	0.817	0.864
3	0.37	0.57	0.644	0.806	0.803	0.880
4	0.34	0.54	0.634	0.788	0.786	0.850
<b>Incongruent</b>						
5*	0.56	0.56	0.06	0.112	0.142	0.269
6*	0.61	0.61	0.056	0.083	0.119	0.240
7	0.16	0.36	0.725	0.697	0.577	0.443
8	0.11	0.31	0.760	0.766	0.651	0.469

**FIGURE S9.** (A) Relative bias and (B) relative mean square error (RMSE) for the posterior mean estimate of  $\theta$  for the SAM prior and robust MAP prior with  $\tilde{w} = 0.5$  (Mix50) and 0.9 (Mix90) in ankylosing spondylitis trial with the dataset from Baeten (2013) excluded. Panel (C) depicts how the weight of the SAM prior self-adapts to prior-data conflict (i.e.,  $\theta - \theta_h$ ). The vertical dotted line indicates  $\theta = \theta_h$ .



## Web Appendix F

### Cutoff $C$ used in simulations

TABLE S7. The calibrated values of cutoff  $C$  in simulations and ankylosing spondylitis trial.

Scenario	NP	SAM	Mix50	PP	CP	SAM 7:3	Mix70	SAM 9:1	Mix90
<b>binary endpoints with <math>\delta = 0.1</math></b>									
Case 1	0.949	0.932	0.925	0.922	0.940	0.931	0.920	0.925	0.920
Case 2	0.949	0.937	0.925	0.923	0.944	0.935	0.923	0.928	0.920
Case 3	0.943	0.939	0.922	0.922	0.947	0.922	0.914	0.917	0.912
<b>normal endpoints</b>									
Case 1	0.948	0.933	0.920	0.919	0.926	0.951	0.947	0.950	0.949
Case 2	0.946	0.936	0.925	0.918	0.928	0.926	0.900	0.919	0.893
Case 3	0.953	0.947	0.934	0.922	0.937	0.956	0.951	0.956	0.953
<b>binary endpoints with <math>\delta = 0.15</math></b>									
Case 1	0.949	0.938	0.922	0.922	0.947	-	-	-	-
Case 2	0.945	0.938	0.923	0.922	0.945	-	-	-	-
Case 3	0.945	0.937	0.928	0.917	0.950	-	-	-	-
<b>survival endpoints</b>									
	0.952	0.910	0.986	-	-	-	-	-	-
<b>Ankylosing spondylitis trial</b>									
Full datasets	0.945	0.944	0.931	-	-	-	-	-	0.923
Exclude Baeten (2013)	0.945	0.943	0.933	-	-	-	-	-	0.930

## Reference

- Baeten D, Baraliakos X, Braun J, Sieper J, Emery P, van der Heijde D, McInnes I, van Laar JM, Landewé R, Wordsworth P, Wollenhaupt J, Kellner H, Paramarta J, Wei J, Brachat A, Bek S, Laurent D, Li Y, Wang YA, Bertolino AP, Gsteiger S, Wright AM, Hueber W. (2013) Antiinterleukin-17A monoclonal antibody secukinumab in treatment of ankylosing spondylitis: a randomised, double-blind, placebo-controlled trial. *Lancet* 382,1705–1713.
- Deodhar AA, Dougados M, Baeten DL, Cheng-Chung Wei J, Geusens P, Readie A, Richards HB, Martin R, Porter B. (2016) Effect of secukinumab on patient-reported outcomes in patients with active ankylosing spondylitis a phase III randomized trial (MEASURE 1). *Arthritis and Rheumatology*, 68, 2901–2910.
- Deodhar A, Poddubnyy D, Pacheco-Tena C, Salvarani C, Lespessailles E, Rahman P, Järvinen P, Sanchez-Burson J, Gaffney K, Lee EB, Krishnan E, Santisteban S, Li X, Zhao F, Carlier H, Reveille JD, COAST-W Study Group. (2019) Efficacy and safety of ixekizumab in the treatment of radiographic axial spondyloarthritis: sixteen-week results from a phase III randomized, double-blind, placebo-controlled trial in patients with prior inadequate response to or intolerance of tumor necrosis factor inhibitors. *Arthritis and Rheumatology*, 71, 599–611.
- Erdes S, Nasonov E, Kunder E et al. (2020) Primary efficacy of netakimab, a novel interleukin-17 inhibitor, in the treatment of active ankylosing spondylitis in adults. *Clin Exp Rheumatol*, 38, 27-34.
- Huang, F., F. Sun, W. Wan, et al. (2019) Secukinumab provides rapid and significant improvement in the signs and symptoms of ankylosing spondylitis: primary (16-week) results from a phase 3 China-centric study, measure 5. *Annals of the Rheumatic Diseases*, 78, 894-895.
- Johnson, V., and Rossell, D. (2010) On the use of non-local prior densities in Bayesian hypothesis tests. *Journal of the Royal Statistical Society: Series B (Statistical Methodology)*, 72, 143-170.
- Kivitz AJ, Wagner U, Dokoupilova E, Supronik J, Martin R, Talloczy Z, Richards HB, Porter B. (2018) Efficacy and safety of secukinumab 150 mg with and without loading regimen in ankylosing spondylitis: 104-week results from MEASURE 4 study. *Rheumatology and Therapy*, 5, 447–462.
- Pavelka, K., A. Kivitz, E. Dokoupilova, et al (2017) Efficacy, safety, and tolerability of secukinumab in patients with active ankylosing spondylitis: a randomized, double-blind phase 3 study, MEASURE 3. *Arthritis Research and Therapy*, 19 (1), 285.

Sieper J, Deodhar A, Marzo-Ortega H, Aelion JA, Blanco R, JuiCheng T, Andersson M, Porter B, Richards HB, MEASURE 2 Study Group. (2017) Secukinumab efficacy in anti-TNF-naive and anti-TNF-experienced subjects with active ankylosing spondylitis: results from the MEASURE 2 study. *Ann Rheum Dis*, 76, 571–575.

van der Heijde D, Cheng-Chung Wei J, Dougados M, Mease P, Deodhar A, Maksymowych WP, van den Bosch F, Sieper J, Tomita T, Landewé R, Zhao F, Krishnan E, Adams DH, Pangallo B, Carlier H, COAST-V study group. (2018) Ixekizumab, an interleukin-17A antagonist in the treatment of ankylosing spondylitis or radiographic axial spondyloarthritis in patients previously untreated with biological disease-modifying anti-rheumatic drugs (COAST-V): 16 week results of a phase 3 randomised, double-blind, activecontrolled and placebo-controlled trial. *Lancet*, 392, 2441–2451.